The Reaction Center−LH1 Antenna Complex of *Rhodobacter sphaeroides* Contains One PufX Molecule Which Is Involved in Dimerization of This Complex

Francesco Francia,[‡] Jun Wang,[‡,§] Giovanni Venturoli,[||] B. Andrea Melandri,[||] Wolfgang P. Barz,*[,‡] and Dieter Oesterhelt*[,‡]

Department of Membrane Biochemistry, Max-Planck-Institute for Biochemistry, 82152 Martinsried, Germany, and Department of Biology, Laboratory of Biochemistry and Biophysics, University of Bologna, Via Irnerio 42, 40126 Bologna, Italy

Received December 8, 1998; Revised Manuscript Received February 2, 1999

ABSTRACT: The PufX membrane protein is essential for photosynthetic growth of *Rhodobacter sphaeroides* wild-type cells. PufX is associated with the reaction center−light harvesting 1 (RC−LH1) core complex and plays a key role in lateral ubiquinone/ubiquinol transfer. We have determined the PufX/RC stoichiometry by quantitative Western blot analysis and RC photobleaching. Independent of copy number effects and growth conditions, one PufX molecule per RC was observed in native membranes as well as in detergent-solubilized RC−LH1 complexes which had been purified over sucrose gradients. Surprisingly, two gradient bands with significantly different sedimentation coefficients were found to have a similar subunit composition, as judged by absorption spectroscopy and protein gel electrophoresis. Gel filtration chromatography and electron microscopy revealed that these membrane complexes represent a monomeric and a dimeric form of the RC−LH1 complex. Since PufX is strictly required for the isolation of dimeric core complexes, we suggest that PufX has a central structural role in forming dimeric RC−LH1 complexes, thus allowing efficient ubiquinone/ubiquinol exchange through the LH1 ring surrounding the RC.

Photosynthetic bacteria are able to convert light energy into chemical energy by the cooperation of membrane-bound pigment−protein complexes. The facultative photosynthetic purple bacterium *Rhodobacter (Rb.)*[1] *sphaeroides* produces an extensive system of intracytoplasmic membranes (ICM) when grown either anaerobically in the light (photosynthetically) or aerobically in the dark under low oxygen partial pressure (semiaerobically) (*1*). The ICM are synthesized from invaginations of the cytoplasmic membrane (*2*) and are functionally differentiated to optimize the photosynthetic energy conversion.

Light energy is transduced in a electrochemical transmembrane potential by the interplay of two large membrane-bound pigment−protein complexes: the photosynthetic reaction center (RC) and the cytochrome (cyt) bc_1 complex. The functional interaction between these two complexes is mediated by a pool of ubiquinone/ubiquinol molecules in the hydrophobic part of the membrane and by soluble cyt c_2 molecules located in the periplasm. Cyclic electron flow through these soluble and membrane-bound molecules generates a proton gradient across the membrane which is utilized for ATP synthesis.

* Corresponding authors. Telephone: +49-89-8578-2344. Fax: +49-89-8578-3557. E-mails: barz@biochem.mpg.de; oesterhelt@biochem.mpg.de.

[‡] Max-Planck-Institute for Biochemistry.

[§] Present address: Department of Chemistry, The Ohio State University, 100 W. 18th Ave., Columbus, OH 43210-1185.

[||] University of Bologna.

[1] Abbreviations: bchl, bacteriochlorophyll *a*; cyt, cytochrome; glygly, glycylglycine; ICM, intracytoplasmic membrane; OG, *n*-octyl-β-D-glucopyranoside; PMC, photosynthetic membrane complex; *Rb*., *Rhodobacter*; RC, reaction center; *Rps*., *Rhodopseudomonas*; *Rs*., *Rhodospirillum*.

The RC is surrounded by two light-harvesting complexes, termed LH1 and LH2, which absorb the light energy and efficiently transfer it to the RC where the charge separation takes place. Both types of antenna complexes are assembled from very similar building blocks. Bacteriochlorophyll *a* (bchl) and carotenoid molecules are noncovalently attached to two hydrophobic low molecular mass (5−7 kDa) apoproteins called α and β, both of which have a single membrane-spanning helix. The apoproteins are present in a 1:1 ratio. The intact antenna structures are oligomers of these α/β pairs and their associated pigments. The LH1 and the RC are present in a fixed stoichiometry in most species of purple bacteria (*3, 4*); the resulting RC−LH1 complex is called the 'core' complex. In contrast, the levels of LH2 antennae vary with irradiance and oxygen tension during growth (*5, 6*). Therefore, the stoichiometry of LH2 and RC−LH1 is strongly dependent on the growth conditions of the cells.

In the past few years, research in this area has been revolutionized by the structural analysis of key protein−pigment complexes involved in the initial steps of photosynthesis. The structure of the RC was determined at atomic resolution in several purple bacteria (*7, 8*). Recently much progress has been achieved in understanding the three-dimensional structure of LH2 complexes of *Rhodopseudomonas* (*Rps.*) *acidophila* (*9*) and *Rhodospirillum* (*Rs.*) *molischianum* (*10*). These complexes have been shown to consist of eight or nine heterodimeric subunits that form a cyclic structure. The α polypeptides form an internal protein ring while the β polypeptides form an external ring, and the B850 bchl molecules are located between these two rings. The structure for the LH1 antenna complex is not yet known at

10.1021/bi982891h CCC: $18.00
Published on Web 04/30/1999

atomic resolution. However, electron microscopy of 2D crystals from several photosynthetic bacteria revealed a ring-like structure of LH1 subunits surrounding a central nucleus attributed to the RC. The structure of LH1 from *Rs. rubrum* was determined at 8.5 Å resolution, clearly showing a symmetrical ring of 16 α/β heterodimer pairs with an external diameter of 116 Å (*11*). From these structural data, a model of the entire photosynthetic unit has been proposed in which the RC−LH1 core complex is surrounded by a variable number of LH2 rings (*12*−*14*). In this model, the bchl molecules of both antenna complexes as well as the bchl special pair (P) of the RC are aligned at the same depth in the membrane, an arrangement that is likely to optimize energy transfer. Very recently, however, evidence has been reported for an incomplete LH1 ring surrounding the RC in native membranes of *Rb. sphaeroides* (*15*). In that study, the structure of the photosynthetic unit was determined at 20 Å resolution using electron microscopy of two-dimensional crystals in their native membrane. The projection map revealed a "S-shaped" structure composed of two incomplete antenna rings, each having a diameter of about 120 Å and containing an electron-dense nucleus attributed to the RC (*15*).

The genes coding for the LH1 subunits (*puf*B and *puf*A) and two of the RC subunits (*puf*L and *puf*M) are located on the so-called *puf* operon and transcribed as part of a polycistronic mRNA. In *Rb. sphaeroides* and *Rb. capsulatus*, the *puf* operon contains an additional gene, termed *puf*X, which encodes a 9 kDa membrane protein, termed PufX, which is essential for photosynthetic growth (*16, 17*). PufX is required for anaerobic, photosynthetic growth of wild-type cells although PufX is not required for *puf* operon expression or primary charge separation in the RC (*18*−*20*). In *Rb. sphaeroides*, PufX is localized in the ICM and is closely associated with the RC−LH1 complex (*16*). A time-dependent assembly study has shown that PufX associates with the RC before the formation of the RC−LH1 core complexes (*21*). Interestingly, the PufX protein has a strong tendency to interact with the α polypeptide of the LH1, while no interaction was detected with the β polypeptide (*22*).

Spontaneous suppressor mutations of a *puf*X deletion strain have been characterized in detail (*23*, *24*). In these strains, photosynthetic competence is restored by spontaneous second site mutations in the plasmid-borne *puf*B or *puf*A genes. These mutations seemed to drastically reduce the levels of LH1 around the RC, thus allowing photosynthetic growth in the absence of PufX. This hypothesis was directly supported by the observation that PufX is not required for photosynthetic growth in the complete absence of LH1 (19). Apparently PufX is only required when the LH1 antenna system is present and when its macromolecular structure around the RC is intact. These observations led to the proposal that PufX facilitates, either directly or indirectly, the flow of ubiquinone/ubiquinol between the RC site and the cyt bc_1 complex (*19*, *20*, *25*).

Recently, in vivo evidence has been presented that PufX is essential for photophosphorylation because it plays a key role in multiple-turnover cyclic electron flow, although it has no apparent role following single-flash excitation (*20*). Under anaerobic conditions, where the oxidized form of ubiquinone is limiting in the ICM, PufX was found to be involved in the lateral, intramembrane exchange of ubiquinone between the RC QB site and the ubiquinone/ubiquinol pool in the membrane (*25*). However, it has not yet been determined whether the function of PufX is direct (e.g., as a ubiquinone carrier protein) or indirect (as a structural organizer of the photosynthetic unit, allowing the diffusion of ubiquinone/ubiquinol through the tight ring of LH1 molecules surrounding the RC).

To distinguish between these possibilities, we further addressed the role of PufX in the RC−LH1 complex. In this study, we investigated the PufX/RC stoichiometry in native ICM and isolated photosynthetic membrane complexes. In addition, we detected a novel membrane complex that is dependent on the presence of PufX. These results point to a structural role of PufX in the supramolecular organization of the photosynthetic unit.

MATERIALS AND METHODS

Materials. DNA-modifying enzymes were from Boehringer Mannheim (Mannheim, Germany). For overexpression of the PufX gene, the QIA*express* Type ATG kit (Qiagen, Hilden, Germany) was used. Nitrocellulose transfer membranes (0.2 μm) for Western blots were purchased from Schleicher & Schuell (Dassel, Germany). All other reagents were from Merck (Darmstadt, Germany) or Sigma Chemical Co. (Munich, Germany) if not indicated otherwise.

Bacterial Growth Conditions. Rb. sphaeroides cultures were grown semiaerobically in Erlenmeyer flasks filled to 50% of the total volume with Sistrom's minimal medium (*26*). The cultures were incubated in darkness at 30 °C and 100 rpm on a gyratory shaker with a displacement radius of 2.5 cm. For photoheterotrophic growth in liquid medium, Schott bottles were fully filled with inoculum and medium. Illumination was provided by far-red light (λ >680 nm) defined by spectral-quality Plexiglas manufactured by Rohm−Haas (Darmstadt, Germany). Semiaerobic or photoheterotrophic growth was monitored using a Klett−Summerson photometer (no. 66 filter) as described previously (*16*). Kanamycin (25 μg/mL) was added to *Rb. sphaeroides* cultures as was tetracycline (2 μg/mL) when plasmid-complemented strains were grown. However, tetracycline was not used for photosynthetic growth to avoid the generation of growth-inhibitory products (*27*).

E. coli strains were grown at 37 °C in Luria broth medium (*28*). Ampicillin (100 μg/mL), kanamycin (25 μg/mL), or tetracycline (10 μg/mL) was used when appropriate. Conjugative transfer of mob$^+$ plasmids into *Rb. sphaeroides* was carried out using *E. coli* S-17 (29) [*rec*A *pro*$^-$ *res*$^-$ *mod*$^+$ Tp^R Sm^R -pRP4-2-Tc::Mu-Km::Tn7] and the diparental filter-mating procedure described previously (*30*). Exconjugants were selected chemoheterotrophically using kanamycin (25 μg/mL) and tetracycline (2 μg/mL).

Recombinant DNA Techniques. A His_6 epitope was added to the carboxyl terminus of *puf*X in the following manner: after digestion of pRKXmut2XT (*16*) with *Bam*HI and *Dra*I (the *Dra*I restriction site is located 128 bp downstream of the *puf*X stop codon), the 4.1 kb *puf* operon construct was isolated and ligated to the 7.3 kb *Bam*HI−*Hin*dIII fragment of pSUP202 (29) which had been linearized with *Hin*dIII, blunt-ended by filling in the overhangs with Klenow polymerase, and digested with *Bam*HI. The resulting plasmid was termed pSUPX. The *puf* operon of pSUPX was subcloned

into pBR322 using *Bam*HI and *Cla*I. After digestion of the resulting plasmid with *Bam*HI and *Ssp*I, the 4.5 kb *puf* operon construct was isolated and cloned into pRK404 (31) which had been linearized with *Hin*dIII, blunt-ended with Klenow polymerase, and digested with *Bam*HI. The resulting plasmid, termed pRKX, carries unique *Hin*dIII and *Cla*I restriction sites on the 5′ and 3′ sides of *puf*X. To insert six histidine residues immediately before the *puf*X stop codon, a two-step PCR approach was used. First, two PCR reactions were performed using pRKX as the template and the following primer pairs: 5′-GGTCTCTCGATCGCCTTCCTCT-3′ (primer 1) and 5′-TCAGTGATGGTGATGGTGATGGAC-GAGATGCTTGATCAGCTCGA-3′ (primer 2) as well as 5′-CTCGTCCATCACCATCACCATCACTGAGACAAGTC-TCGGGGCAGGG-3′ (primer 3) and 5′-AGCGGATAA-CAATTTCACACAGGA-3′ (primer 4). Aliquots of both PCR products were mixed and used as the template for a second PCR primed with primer 1 and primer 4. The resulting PCR fragment was digested with *Hin*dIII and *Cla*I and ligated into the *Hin*dIII and *Cla*I sites pRKX, thereby replacing the untagged *puf*X gene with His_6-tagged *puf*X. The resulting plasmid was termed $pRKXHis_6$. Sequence analysis confirmed the expected sequence for the His_6-tagged *puf*X gene of $pRKXHis_6$.

To integrate the *puf* operon carrying the His_6-tagged *puf*X gene into the chromosome of the green *puf* deletion strain ΔQ-X/g (*20*), a suitable suicide plasmid (termed $pSUPtetX-His_6$) was constructed in the following manner: Using *Bam*HI and *Cla*I, the untagged *puf* operon of pSUPX was replaced with the corresponding His_6-tagged *puf* operon of $pRKXHis_6$. A tetracycline resistance gene was cloned into the resulting plasmid, $pSUPXHis_6$, to allow the selection of single-crossover events between the suicide plasmid and the chromosome of *Rb. sphaeroides*. To this end, the 1.4 kb *Eco*RI−*Ava*I fragment of pBR322 was ligated with the 3.4 kb *Eco*RI−*Ava*I fragment of pSUP202 (29). The resulting plasmid, termed pSUPtet, was linearized with *Eco*RI and ligated with the 6.8 kb *Eco*RI fragment of $pSUPXHis_6$. The resulting suicide plasmid, $pSUPtetXHis_6$, was analyzed by restriction analysis. Conjugation of $pSUPtetXHis_6$ into the *puf* deletion strain ΔQ-X/g (*20*) resulted in a strain termed $PUFXHis_6$ which carries the complete *puf* operon (including the His_6-tagged *puf*X) in its correct chromosomal location. Southern blot analysis confirmed the expected genetic structure of the *puf* operon in $PUFXHis_6$.

To overexpress and purify PufX-His_6 from *E. coli*, the tagged *puf*X gene was cloned into pQE-70 (Qiagen, Hilden, Germany). To this end, the epitope-tagged *puf*X gene was amplified by PCR using $pRKXHis_6$ as the template and the oligonucleotides 5′-TGAGGAAAGCTTACCATGGCTGA-CA-3′ and 5′-CCGAGACTTAGATCTGACGAGATGCTT-3′. The resulting PCR product was digested with *Nla*III (compatible with *Sph*I) and *Bgl*II and inserted into pQE-70 digested with *Sph*I and *Bgl*II. The resulting construct, termed $pQE-70XHis_6$, encodes a fusion protein composed of the 82 amino acid PufX protein followed by 1 serine and 6 histidine residues (termed PufX-His_6).

Overexpression and Purification of His_6-Tagged PufX from E. coli. $pQE-70XHis_6$ was transformed into *E. coli* host strain M15 carrying the pREP4 repressor plasmid, which is compatible with all plasmids carrying the ColE1 origin of replication.

Two liter cultures of *E. coli* strain M15 harboring both plasmids were grown at 37 °C in the presence of ampicillin (200 μg/mL) and kanamycin (25 μg/mL) until A_{600} reached 0.7−0.9. The expression of protein was induced by 500 mM IPTG. The culture was switched to 30 °C and incubated for 4 h. The cells were harvested by centrifugation, and the pellet was suspended in 20 mL of sonication buffer (50 mM Tris, 100 mM NaCl, 10% v/v glycerol, pH 8.0). The cells were lysed with lysozyme (1 mg/mL) in the presence of DNase (5 μg/mL) and RNase (10 μg/mL) on ice for 30 min. The cell suspension was sonicated using a Branson microtip at 50% capacity, setting 5 for 5 min. The cell lysate was centrifuged at 11000*g* for 15 min, and the supernatant was centrifuged at 190000*g* for 1.5 h. The membrane pellet was resuspended in solubilization buffer (50 mM Tris, 100 mM NaCl, 10% v/v glycerol, pH 8.0) containing 1.5% (w/v) *n*-octyl-β-D-glucopyranoside (OG) at a protein concentration of ∼4−5 mg/mL. Following solubilization for 1 h on ice, the suspension was centrifuged at 250000*g* for 20 min to remove any unsolubilized portion. Then 4 mL of a 50% slurry of Ni−NTA, previously equilibrated with solubilization buffer, was added to the supernatant, and stirred for 60 min. The slurry was loaded onto an empty column and washed with solubilization buffer until the A_{280} of the flow-through was lower than 0.01. The column was washed with wash buffer [50 mM NaH_2PO_4, 10 mM Tris, 100 mM NaCl, 10% (v/v) glycerol, 0.8% (w/v) OG, pH 6.3] until the A_{280} of the flow-through was lower than 0.01. The His_6-tagged PufX protein was eluted with elution buffer [50 mM NaH_2PO_4, 10 mM Tris, 100 mM NaCl, 10% glycerol (v/v), 0.8% (w/v) OG, pH 4.5]. The purity and identity of the purified protein were confirmed by SDS−PAGE and sequence analysis. PufX protein sequencing was performed with a Procise 492 amino acid sequencer with a PTH Analyzer 140C and a UV detector 785A (Applied Biosystems, Weiterstadt, Germany).

The concentration of purified PufX-His_6 was analyzed using a 6300 Amino acid analyzer (Beckman, Munich, Germany). Following complete hydrolysis of the protein, the concentration of each amino acid was determined using the analysis software provided by the manufacturer (System Gold, Beckman). The concentration of PufX-His_6 was calculated on the basis of the amino acid sequence. To allow calculation of the error associated with the determination of the protein concentration (see below), the entire procedure was performed 3 times.

ICM Isolation and Analysis. Chromatophores (ICM) were isolated from semiaerobically or photoheterotrophically grown cells as described previously (*32*). Protein concentrations of the isolated ICM were determined using the BCA Protein Assay Reagent following the manufacturer's instructions (Pierce, Rockford, IL). An aliquot of ICM was extracted with acetone−methanol (7:2 v/v). After centrifugation, the protein pellet was dissolved in 0.1 M NaOH−1% SDS for concentration determination.

Western Blot Detection of PufX-His_6. SDS−polyacrylamide gel electrophoresis (SDS−PAGE) was carried out using the tricine buffer system as described by Schägger and von Jagow (*32*). We used a 15.5% acrylamide−1% bisacrylamide gel, and 6 M urea was included in the separating gel to improve the resolution. Before electrophoresis, the ICM samples were solubilized with 3% OG at a protein concen-

tration of 2 mg/mL for 30 min at room temperature. After addition of loading buffers, the samples were heated at 60 °C for 30 min.

Protein transfer to nitrocellulose membranes (Schleicher & Schuell, Dassel, Germany) was carried out in 50 mM Tris, 95 mM glycine, and 0.005% SDS using a semi-dry Western blot apparatus (LKB, Piscataway, NJ). Immunodetection was performed using an ECL Western blotting system as suggested by the manufacturer (Amersham, Braunschweig, Germany). The polyclonal anti-His_6 primary antibody (ICN, Aurora, OH) was used at a final dilution of 1:1000. Goat anti-rabbit antibody coupled with horseradish peroxidase was purchased from Nordic Immunological Laboratories (Tilburg, The Netherlands) and used at a 1:10 000 dilution.

To quantitatively determine the concentration of PufX-His_6 in ICM or solubilized membrane complexes, Western blots were performed in parallel with these samples and with known amounts of purified PufX-His_6 as a standard (see Figure 1). Care was taken that the integrated intensities of the protein standard were in the linear range. The sizes of the sample aliquots were chosen in a way that their ECL signals were within the range of signals of the calibration curve. Suitable ECL exposures were scanned with a densitometer, and the protein concentration was calculated for each sample by comparison with the calibration curve of purified PufX-His_6. At least four Western blots were performed for each sample. The uncertainty associated with this quantitation procedure was calculated as described below.

Isolation of Photosynthetic Membrane Complexes. Photosynthetic membrane complexes (PMCs) were solubilized and purified using a previously described method (*34*) with the following two modifications: first, the first membrane extraction step (after the NaBr wash) was performed with a final OG concentration of 0.75% w/v. After centrifugation at 175000*g* for 90 min, the pellet was resuspended in 50 mM glygly, 1% OG, pH 7.8, to a protein concentration of 10 mg/mL and extracted with 3% OG and 0.5% sodium cholate as described before (*34*). Second, the sucrose density gradient contains 0.6% OG, 0.2% sodium cholate instead of 1% OG, 0.25% sodium cholate. Following isolation of the PMCs, the sucrose was removed by gel filtration through a Sephadex G-25 column (PD 10, Pharmacia, Uppsala, Sweden) previously equilibrated with the buffer 0.6% OG, 0.2% sodium cholate, 50 mM glygly, pH 7.8. When appropriate, the sugar-free PMCs were concentrated by ultracentrifugation using a Centricon 100 microconcentrator (100 kDa cutoff) following the instructions of the manufacturer (Amicon, Witten, Germany). The entire purification procedure was performed at 4 °C or in an ice bath.

Determination of the bchl Concentration. Total bchl was extracted from the PMCs by adding aliquots of 50, 80, and 100 μL to 1 mL of an acetone−methanol mixture (7:2 v/v). Following centrifugation (15 min at 4 °C) in an Eppendorf microcentrifuge, the absorbance of the supernatant was measured at 772 nm and the bchl concentration determined as described before (*35*). In all cases, the three aliquots (50, 80, and 100 μL) gave a linear curve. In addition, the absorption maximum was detected at the same wavelength in all three samples.

Determination of the Critical Micellar Concentration (CMC). The CMC is the lowest concentration at which detergents or other amphiphilic molecules aggregate to form micelles. To experimentally determine the CMC of OG in the presence of 0.2% (w/v) sodium cholate, we studied the incorporation of iodine into micelles built from mixes of these two detergents. This method is based on the fact that the absorption of iodine at 360 nm rises drastically upon its incorporation into the hydrophobic core of the micelles. Aqueous solutions of 0.2% (w/v) sodium cholate and increasing concentrations of OG (ranging from 0 to 1.5% w/v) were made. Following the addition of 0.1 volume of a saturated solution of iodine in 13% (v/v) ethanol, the samples were vortexed and incubated at 4 °C for 10 min before measuring the absorbance at 360 nm. The absorbance values were plotted against the percentage of OG, and the CMC was estimated from the intercept of the two linear curves below and above the CMC. In the presence of 0.2% (w/v) sodium cholate, the CMC of OG is equal to 0.35% (w/v).

Determination of the Reaction Center Concentrations. To evaluate the concentration of photoactive RC in the ICM or in isolated membrane complexes, flash-induced photobleaching of the primary electron donor (P) of the RC was measured spectrophotometrically. ICM samples were diluted with 50 mM MOPS, 100 mM KCl, pH 7.0, to final bchl concentrations ranging from 16 to 40 μM. The cyt bc_1 complex was inhibited with 10 μM antimycin A; 10 μM valinomycin and 10 μM nigericin were also added to collapse the transmembrane proton gradient and to avoid spectral interference due to bchl and carotenoid electrochromic effects. Measurements were performed in an argon atmosphere under controlled redox conditions, as described previously (*36*). 1,2-Naphthoquinone and *p*-benzoquinone (10 μM each) were used as redox mediators, and the ambient redox potential (E_h) was poised at 180 ± 15 mV. Flash-induced absorption changes were monitored at 542 and 605 nm (*37*, *38*). Actinic flashes of light, approximately 10 μs half-width, were provided by a xenon lamp (3.2 J discharge energy; EG&G, Electro Optics, Salem, MA) screened through two layers of Wratten 88A gelatin filters (Kodak). The spectrophotometric signals were recorded using a single-beam kinetic spectrophotometer of local design (time resolution 0.1 μs; bandwidth less than 2 nm) interfaced with a LeCroy 9410 digital oscilloscope. Trains of 10 flashes spaced 40 ms apart were used to fully oxidize the RC, and the signal was averaged 10 times. The dark time between the excitation trains of flashes was 60 s.

The isolated photosynthetic membrane complexes (PMCs) were frozen in liquid nitrogen immediately after isolation, and thawed just before the RC determinations. The total concentration of photooxidizable reaction centers was measured following essentially the procedure described above, except that PMC samples were placed in an open unstirred cuvette supplemented with 1 mM sodium ascorbate.

Gel Filtration Chromatography. Isolated photosynthetic membrane complexes were injected in a Superose 6 column (Pharmacia Superose 6 HR, 10/30) and eluted at 0.5 mL/min flow by an Äkta Explorer 100 System (Pharmacia) in a cold chamber. Elution peaks were detected at 280, 456, and 560 nm. To construct a calibration curve, purified carbonic anhydrase (29 kDa), alcohol dehydrogenase (150 kDa), thyroglobulin (669 kDa), and Blue Dextran (2000 kDa) (Sigma, Munich, Germany) were injected together at an individual concentration of 1 mg/mL and analyzed as described above.

Electron Microscopy. Freshly isolated photosynthetic complexes were prepared for electron microscopy as described elsewhere (*39*), except that the PMCs were fixed with 10 mM glutaraldehyde for 15 min before adsorption onto the grid. Following washing with 50 mM glycylglycine, pH 7.8, the samples were stained with 2% uranyl acetate. Electron microscopy was performed with a Philips EM420 electron microscope at a magnification of 48000*x*.

Estimate of Errors. The following sources of uncertainty have been considered in quantitatively determining the concentration of PufX-His_6 in ICM and isolated PMCs:

(a) Quantitation of PufX-His_6 by Protein Hydrolysis. The concentration of purified PufX-His_6 used for calibrating Western blots was determined 3 times by complete hydrolysis. In each quantitation experiment, 13 determinations were performed, based on the amino acid composition of PufX-His_6. The weighted mean and the corresponding standard deviation were calculated.

(b) Calibration of Western Blots. For each experiment, a correlation plot (picomoles of purified PufX-His_6 vs signal intensity) was constructed and a linear fit performed, weighted according to the uncertainties in picomoles of PufX-His_6 estimated in (a). The uncertainty associated with the quantitation of PufX-His_6 in ICM or PMC samples was evaluated from the standard deviations of the fitting parameters in the correspondent calibration (*40*).

(c) Dilution of the Samples in Running Western Blot Experiments. The errors resulting from the previous points have been combined with errors in the volumes (buffer and sample) when preparing the diluted sample for Western blotting, resulting in the PufX concentration in the original preparation for each Western blot experiment. Standard error propagation procedures have been used in this as well as in other steps of error evaluation (*40*). Usually this source of uncertainty does not contribute substantially to that of the final result, but can be important at high dilution.

(d) Combination of Results from Western Blot Experiments Performed with a Given Preparation (at Least Four Independent Experiments for Each ICM Preparation, Two Independent Experiments for Each PMC). The weighted mean and the resulting standard deviation have been calculated from the results of (c) for each preparation.

The error in the concentration of RC has been estimated by assuming an uncertainty equal to one-fifth of the peak-to-peak noise in reading spectrophotometric signals and by considering dilution errors. Finally, in evaluating PufX/RC and bchl/RC ratios, the propagation of uncertainties in PufX, RC, and bchl concentrations, estimated as described above, has been taken into account.

RESULTS

Determination of the PufX/RC Stoichiometry in Native ICM. The integral membrane protein PufX is required for light-driven cyclic electron flow of *Rb. sphaeroides* wild-type cells (*20*, *25*). Interestingly, PufX is physically associated with the RC−LH1 complex (*16*), indicating that it is involved in facilitating the functional interaction of the components of the photosynthetic unit. To better understand the molecular function of PufX, we studied the number of PufX molecules contained in each RC−LH1 core complex. In a first approach, the PufX/RC stoichiometry was determined in isolated ICM. The concentration of the PufX was measured by quantitative Western blot analysis, while the RC was quantitated using photobleaching techniques (see below).

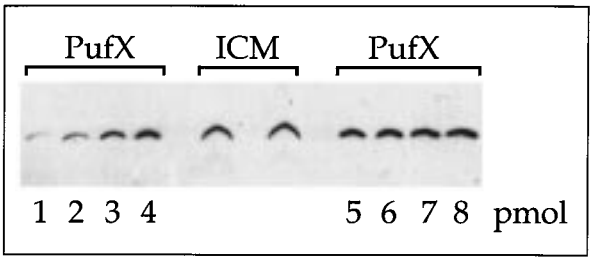

FIGURE 1: Quantitative determination of the PufX concentration using Western blot analysis. ICM were isolated from photosynthetically grown PUFXHis$_6$ cells. Two aliquots of membranes containing 4.4 pmol of RC (labeled ICM) and the indicated amounts of purified PufX-His_6 (labeled PufX) were separated by SDS−PAGE and analyzed by Western blotting using anti-His_6 antibodies. The shape of the PufX band in the ICM samples is due to the presence of lipids and carotenoids.

To allow quantitation of PufX in isolated ICM, their Western blot signals were compared to that of isolated PufX protein. To this end, we constructed a *puf*X allele that encodes a PufX protein with a carboxyl-terminal histidine tag (see Materials and Methods). This epitope-tagged protein, PufX-His_6, is functional as judged by its ability to complement the growth defect of a *Rb. sphaeroides* strain lacking *puf*X (not shown). PufX-His_6 was overexpressed from *E. coli* and purified using Ni−NTA chromatography (see Materials and Methods). The resulting PufX-His_6 preparation was pure as judged by SDS−PAGE and Coomassie-staining and free of further His_6 epitopes as seen by Western blot analysis using anti-His_6 antibodies (not shown).

A green strain of *Rb. sphaeroides* lacking the whole *puf* operon by substitution of a kanamycin resistance gene, ΔQ-X/g (*23*), was complemented with the plasmid pRKXHis$_6$ (see Materials and Methods). Since the expression of plasmid-borne genes can be influenced by the plasmid's copy number and by cis-acting elements that are known to regulate the expression of the *puf* operon (*41*, *20*), the PufX/RC stoichiometry was also studied in a strain carrying a single, chromosomal copy of the *puf* operon (including the His_6-tagged *puf*X gene). To this end, the *puf* operon of pRKXHis$_6$ was integrated into the chromosome of the *puf* deletion strain ΔQ-X/g (see Materials and Methods). The resulting strain, termed PUFXHis$_6$, carries the complete *puf* operon (with the C-terminal His_6-tag) in its correct chromosomal location. Both of these strains were grown photosynthetically as well as semiaerobically in the dark, and the ICM were isolated by French press disruption.

To quantitatively determine the PufX concentration in these ICM preparations, small aliquots were analyzed by Western blot analysis using anti-His_6 antibodies. For quantitative comparison, known amounts of purified PufX-His_6 were analyzed in parallel. Figure 1 shows a typical Western blot with two identical aliquots of ICM (lanes 5 and 6) and increasing amounts of purified PufX-His_6 (lanes 1−4 and lanes 7−10). The different shapes of the PufX bands that are observed for the purified and ICM-bound PufX-His_6 can be attributed to the lipids and pigments present in the latter samples.

Table 1: Stoichiometry of PufX per RC in Isolated ICM Preparations[a]

strain	growth conditions	PufX/RC
ΔQ-X/g (pRKXHis$_6$)	semiaerobic	0.99 ± 0.07
ΔQ-X/g (pRKXHis$_6$)	photosynthetic	0.83 ± 0.21
PUFXHis$_6$	semiaerobic	0.86 ± 0.14
PUFXHis$_6$	photosynthetic	0.86 ± 0.15

[a] The concentration of PufX-His$_6$ was determined by quantitative Western blot analysis using anti-His$_6$ antibodies; the RC was quantified using flash-induced photooxidation of the primary electron donor P (see Materials and Methods).

To determine the PufX/RC stoichiometry in the ICM preparations, the RC concentration was measured by monitoring the photooxidation of the primary electron donor induced by trains of actinic flashes. Flash-induced absorbance changes were recorded at 542 and 605 nm, and the RC concentrations were calculated using a differential extinction coefficient of $\epsilon_{542-605} = 29.8\ mM^{-1}\ cm^{-1}$ (*37*, *38*).

As shown in Table 1, the number of PufX molecules per RC is independent of the strain and growth condition used. Taken together, these data clearly show that native ICM contain one PufX molecule per RC−LH1 complex.

Isolation of Photosynthetic Membrane Complexes. To confirm the observed PufX/RC stoichiometry in isolated RC−LH1 complexes, photosynthetic membrane complexes (PMCs) were isolated from ΔQ-X (pRKXHis$_6$) cells. In addition, a well-characterized *puf*X-deleted mutant, ΔQ-X/g (p2T) (*23*), was included in these studies to further characterize the role of PufX in the RC−LH1. The only difference between this mutant and ΔQ-X/g (pRKXHis$_6$) is the absence or presence of the His$_6$-tagged *puf*X gene.

PMCs were isolated from ICM preparations of these strains by using a differential solubilization protocol (see Materials and Methods). After removal of peripheral membrane proteins with sodium bromide and extraction of the membranes with 0.75% *n*-octyl-*β*-D-glucopyranoside (OG), RC−LH1 complexes were solubilized using 3% OG and 0.5% sodium cholate. Following removal of membranes by ultracentrifugation, the detergent extract was separated by zone centrifugation using a sucrose density gradient (10−40% w/w sucrose) containing 0.6% OG and 0.2% sodium cholate. This centrifugation technique separates macromolecules according to their sedimentation coefficients.

As shown in Figure 2, the gradients obtained from ΔQ-X/g (pRKXHis$_6$) (left tube) and ΔQ-X/g (p2T) (right tube) contain several green bands known to consist of PMCs (*34*). The relative intensity of the bands depends on the growth conditions and growth phase of the cells from which the ICM were isolated (not shown). In both cases, one band is present at the very top of the gradient. This fraction consists mainly of free carotenoid as detected by absorption spectra and RC photobleaching (not shown).

Three additional PMC bands are present in both gradients shown in Figure 2. With increasing density, PMCs isolated from ΔQ-X/g (pRKXHis$_6$) are termed PMC1$_{WT}$, PMC2$_{WT}$, and PMC3$_{WT}$. Similarly, PMCs isolated from ΔQ-X/g (p2T) are termed PMC1$_{\Delta X}$, PMC2$_{\Delta X}$, and PMC3$_{\Delta X}$, respectively. Interestingly, under all growth conditions (semiaerobically or photosynthetically) and in all growth phases tested, a fourth green band at higher density (termed PMC4$_{WT}$) was always obtained from detergent-solubilized ICM isolated

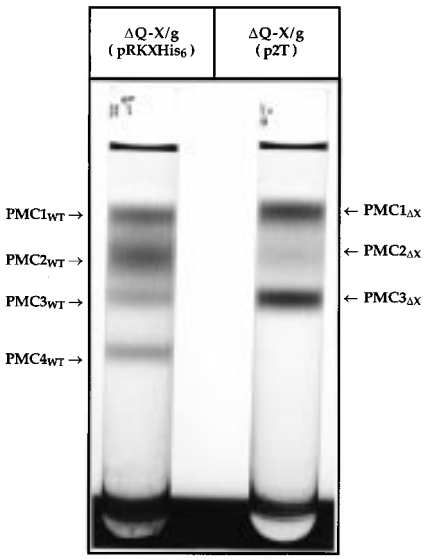

FIGURE 2: Rate zonal centrifugation of detergent extracts. ICM were isolated from semiaerobically grown cells and solubilized with 3% OG, 0.5% sodium cholate as described under Materials and Methods. The detergent extracts were separated on 10−40% (w/w) sucrose density gradients containing 0.6% OG, 0.2% sodium cholate in 50 mM glygly, pH 7.8. Left tube, photosynthetic membrane complexes (PMCs) from ΔQ-X/g (pRKXHis$_6$) cells (containing *puf*X); right tube, PMCs from ΔQ-X/g (p2T) cells (lacking *puf*X).

from ΔQ-X/g (pRKXHis$_6$), but never from those isolated from ΔQ-X/g (p2T) cells. The lack of PMC4 in the absence of *puf*X suggests that PufX is required for the formation or stability of this membrane complex. PMC4 was also isolated from ΔQ-X (pRKX) lacking a His$_6$ tag, indicating that the presence of this band was not due to the His$_6$ tag added to the PufX protein (not shown).

Characterization of a Novel Membrane Complex Requiring pufX. To determine the subunit composition of the PMCs isolated from ΔQ-X/g (pRKXHis$_6$) and ΔQ-X/g (p2T), the green fractions were collected from sucrose density gradients such as those shown in Figure 2 and characterized by absorption spectroscopy, SDS−PAGE, and Western blotting.

Figure 3A shows the absorption spectrum of native ICM isolated from ΔQ-X/g (pRKXHis$_6$). The spectrum shows the characteristic absorption bands of carotenoids (400−500 nm) and absorption peaks that are due to the overlapping bchl peaks of RC, LH1, and LH2 complexes (750−900 nm). Figure 3B shows the spectrum of identical ICM after detergent extraction with OG. Except for a better resolution of the peaks at 850 nm (LH2) and 875 nm (LH1), the spectrum is very similar to that of untreated ICM, demonstrating that the integrity of the PMCs was not significantly altered by the solubilization from the membrane. Especially the absence of an absorption peak at 820 nm, the absorption maximum of the minimum building block of the LH1 complex (composed of $\alpha_1\beta_1$ heterodimers), shows that the antenna complexes are not significantly decomposed by the solubilization procedure. Such a decay of LH1 antenna into its minimum building block has been observed in *Rs. rubrum* where extraction of the membrane with high OG concentration caused a blue shift of the LH1 peak from 872 to 820 nm (*42*).

Absorption spectra were recorded for the PMCs isolated from ΔQ-X/g (pRKXHis$_6$) and ΔQ-X/g (p2T). As shown in

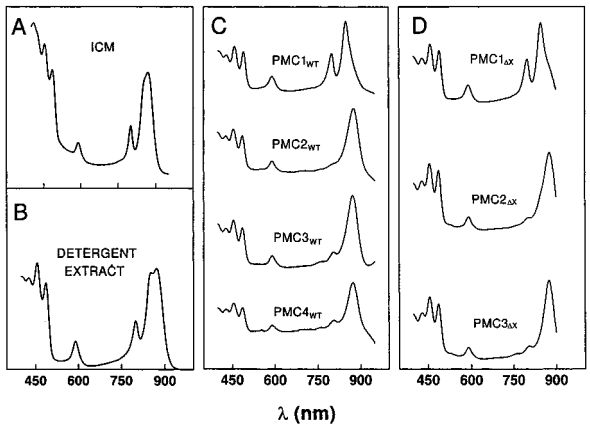

FIGURE 3: Absorption spectra of isolated ICM, detergent extract, and isolated PMCs. ICM were isolated from semiaerobically grown cells of ΔQ-X/g (pRKXHis$_6$) (panels A−C) and ΔQ-X/g (p2T) (panel D), extracted with 3% OG, 0.5% sodium cholate, and separated over a 10−40% (w/w) sucrose density gradient containing 0.6% OG and 0.2% sodium cholate. The absorption spectra were normalized to the absorption maximum of the carotenoids and displaced vertically from each other for clarity. (A) Isolated ICM; (B) supernatant of the centrifugation after detergent extraction; (C) PMCs isolated from ΔQ-X/g (pRKXHis$_6$); (D) PMCs isolated from ΔQ-X/g (p2T).

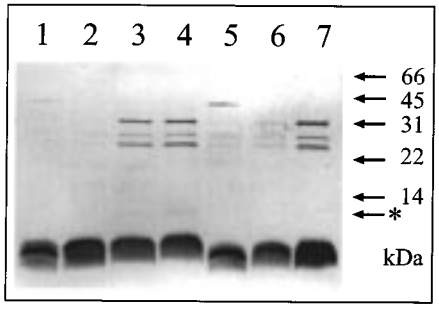

FIGURE 4: Silver-stained SDS−polyacrylamide gel of isolated PMCs. Isolated PMCs from semiaerobically grown cells of ΔQ-X/g (pRKXHis$_6$) and ΔQ-X/g (p2T) were separated by SDS−PAGE using the tricine buffer system of Schägger and von Jagow (*32*). A total of 0.1 μg of protein was loaded onto each lane. Lane 1, PMC1$_{WT}$; lane 2, PMC2$_{WT}$; lane 3, PMC3$_{WT}$; lane 4, PMC4$_{WT}$; lane 5, PMC1$_{\Delta X}$; lane 6, PMC2$_{\Delta X}$; lane 7, PMC3$_{\Delta X}$. The positions of molecular mass markers are indicated. The star indicates the very faint band of PufX-His$_6$ in lanes 3 and 4 (better visible on the original gel).

Figure 3C,D, PMC1$_{WT}$ and PMC1$_{\Delta X}$ have the typical absorption profile of LH2 complexes with two major peaks at 800 and 850 nm. In contrast, PMC2$_{WT}$ and PMC2$_{\Delta X}$ have a prominent near-IR absorption peak at 875 nm, suggesting that they are composed of LH1 complexes. In addition, minor absorption maxima at 760 and 800 nm indicate that PMC2$_{WT}$ and PMC2$_{\Delta X}$ may contain trace amounts of RC. Finally, PMC3$_{WT}$, PMC3$_{\Delta X}$, and PMC4$_{WT}$ show absorption profiles that are characteristic of the RC−LH1 complex (absorption peaks at 760, 800, and 875 nm). Therefore, the subunit composition of PMC3$_{WT}$ and PMC4$_{WT}$ appears to be very similar despite their different sedimentation coefficients.

To confirm the spectroscopic analysis of PMCs, the protein content of the PMCs from ΔQ-X/g (pRKXHis$_6$) and ΔQ-X/g (p2T) was analyzed by SDS−PAGE followed by silver staining. The gel is presented in Figure 4. The protein pattern in lanes 1 and 5 confirms that PMC1$_{WT}$ and PMC1$_{\Delta X}$ contain mainly low molecular mass polypeptides (<10 kDa), consistent with the interpretation that they are composed of LH2 antennae. Primarily small proteins were also observed in lanes 2 and 6, suggesting that PMC2$_{WT}$ and PMC2$_{\Delta X}$ are mainly composed of LH1 complexes. Very small amounts of the three RC subunits (25−30 kDa) were also detectable in PMC2$_{WT}$ and PMC2$_{\Delta X}$. As shown in lanes 3, 4, and 7 of Figure 4, PMC3$_{WT}$, PMC3$_{\Delta X}$, and PMC4$_{WT}$ are also composed of RC and LH1 subunits. Interestingly, the LH1/RC stoichiometry is significantly smaller in these PMCs when compared to PMC2$_{WT}$ and PMC2$_{\Delta X}$. Since equivalent amounts of total protein were loaded onto each lane in Figure 4, these results suggest that PMC2$_{WT}$ and PMC2$_{\Delta X}$ are mainly constituted of LH1 with only traces of RC ("empty rings" of LH1), whereas PMC3$_{WT}$, PMC3$_{\Delta X}$, and PMC4$_{WT}$ appear to be RC−LH1 core complexes. Moreover, a weak band in the 10 kDa region, attributable to PufX, was only observed in PMC3$_{WT}$ and PMC4$_{WT}$ and is faintly visible in lanes 3 and 4 for Figure 4. However, the PufX-His$_6$ band was clearly visible in all Western blot performed for the stoichiometry determination (not shown).

Table 2: PufX/RC and bchl/RC Stoichiometry in Isolated PMCs[a]

PMC	bchl/RC	PufX/RC
PMC1$_{WT}$	224 ± 19	nd
PMC2$_{WT}$	180 ± 9	2.03 ± 0.12
PMC3$_{WT}$	36.7 ± 1.3	0.87 ± 0.16
PMC4$_{WT}$	30.8 ± 1.6	0.76 ± 0.15
PMC1$_{\Delta X}$	116 ± 15	nd
PMC2$_{\Delta X}$	165 ± 16	nd
PMC3$_{\Delta X}$	39.6 ± 2.6	nd

[a] PMCs were isolated from semiaerobically grown cells of ΔQ-X/g (pRKXHis$_6$) and ΔQ-X/g (p2T). The concentrations of bchl, PufX, and RC and the corresponding errors were evaluated as described under Materials and Methods. For each sample, at least two independent determinations of bchl, PufX, and RC were performed.

Stoichiometric bchl/RC Ratio in Isolated Membrane Complexes. The bchl/RC ratio was determined for the isolated PMCs to quantitatively confirm that PMC3$_{WT}$, PMC3$_{\Delta X}$, and PMC4$_{WT}$ have the characteristic stoichiometry of the RC−LH1 complex. To this end, the RC concentration was evaluated by photooxidation of the primary donor (see Materials and Methods). We found that PMC3, PMC4, and ICM displayed very similar levels of saturation in RC photobleaching experiments using trains of flashes (approximately 90% after the first of 10 actinic flashes; not shown). A $\Delta\epsilon_{605-542} = 29.8$ mM^{-1} cm^{-1} was used for determining the RC concentration (*37*, *38*).

At the end of the photobleaching experiment, bchl was extracted from the PMCs and quantitatively determined at 772 nm (see Materials and Methods). Table 2 shows the stoichiometric bchl/RC ratio for the isolated PMCs. A considerable amount of RC was detected in every PMC, but PMC1$_{WT}$, PMC1$_{\Delta X}$, PMC2$_{WT}$, and PMC2$_{\Delta X}$ have a bchl/RC ratio that cannot be assigned to any known membrane complex. Instead, these values are likely to be caused by traces of RC that are associated with solubilized LH2 and LH1 complexes, respectively. In contrast, PMC3$_{WT}$, PMC3$_{\Delta X}$, and PMC4$_{WT}$ display bchl/RC stoichiometries similar to the value expected for purified RC−LH1 complexes (see Discussion).

PufX/RC Stoichiometry in Isolated Membrane Complexes. To confirm the stoichiometric PufX/RC ratio observed for

native ICM, similar determinations were performed for isolated $PMC2_{WT}$, $PMC3_{WT}$, and $PMC4_{WT}$ (see Table 2). In $PMC2_{WT}$, the PufX/RC stoichiometry is around 2, suggesting that more RC than PufX is removed from the RC−LH1 complex by the detergent extraction.

Interestingly, both $PMC3_{WT}$ and $PMC4_{WT}$ have a stoichiometric PufX/RC ratio close to 1. These results are in good agreement with the bchl/RC ratio in the PMCs and again confirm that these PMCs have a nearly identical subunit composition despite their different positions in the sucrose density gradients. Since rate zonal centrifugation used to isolate the PMCs separates macromolecules according to their sedimentation coefficients (in contrast to isopycnic centrifugation which separates according to density), $PMC3_{WT}$ and $PMC4_{WT}$ have drastically different sedimentation coefficients. Therefore, $PMC3_{WT}$ and $PMC4_{WT}$ most likely have significant differences in their molecular weight and/or shape.

$PMC4_{WT}$ Is a Dimeric Form of $PMC3_{WT}$. One possible way to explain the observed differences in sedimentation of $PMC3_{WT}$ and $PMC4_{WT}$ would be that $PMC4_{WT}$ is an oligomeric form of $PMC3_{WT}$. To test this hypothesis and to quantitatively determine the oligomerization level, $PMC3_{WT}$, $PMC3_{\Delta X}$, and $PMC4_{WT}$ were analyzed by gel filtration chromatography. A Superose 6 column was used in the presence of 0.6% OG and 0.2% sodium cholate. First, a set of molecular mass standards was injected to obtain a calibration curve (see Materials and Methods). Next, separate runs were performed with isolated PMCs. $PMC4_{WT}$, $PMC3_{WT}$, and $PMC3_{\Delta X}$ have apparent molecular masses of 750, 472, and 445 kDa, respectively (not shown). The ratio of the apparent masses of $PMC4_{WT}$ and $PMC3_{WT}$ is 1.59, whereas $PMC3_{WT}$ and $PMC3_{\Delta X}$ have a ratio of 1.06. Therefore, $PMC3_{WT}$ and $PMC3_{\Delta X}$ are very similar in their apparent mass, whereas $PMC4_{WT}$ is considerably larger than $PMC3_{WT}$. Although the ratio between $PMC4_{WT}$ and $PMC3_{WT}$ is not equal to 2 $PMC4_{WT}$ is likely to be a dimeric form of $PMC3_{WT}$ (see Discussion).

To demonstrate the dimeric nature of $PMC4_{WT}$ directly, freshly isolated $PMC3_{WT}$ and $PMC4_{WT}$ were subjected to electron microscopy (see Materials and Methods). Figure 5A,B shows negatively stained micrographs of these PMCs. As shown in Figure 5A, $PMC3_{WT}$ contains a variety of circular and rectangular structures. Since $PMC3_{WT}$ is likely to bind to the grid in different orientations, these structures may represent top views and side views of the RC−LH1 complexes. Consistent with this interpretation, the circular structures in Figure 5A have a diameter of 11.5−12.0 nm, a value which is in good agreement with values previously described for the diameter of the core complex (*11*, *39*). Therefore, this circular structure is most likely composed of a ring of LH1 surrounding the RC.

As shown in Figure 5B, the electron micrographs of $PMC4_{WT}$ also show circular and rectangular structures similar to those in Figure 5A. In addition, $PMC4_{WT}$ also contains a significant number of larger structures with a shape similar to that of the number eight. Interestingly, this structure appears to consist of two intertwined circles each having a diameter of approximately 12 nm. Therefore, we propose that $PMC4_{WT}$ is a membrane complex composed of two intertwined rings of LH1 containing two RCs and two PufX molecules. Since this dimeric core complex was isolated only from membranes containing PufX, we propose that PufX plays an essential structural role in organizing this macromolecular membrane complex.

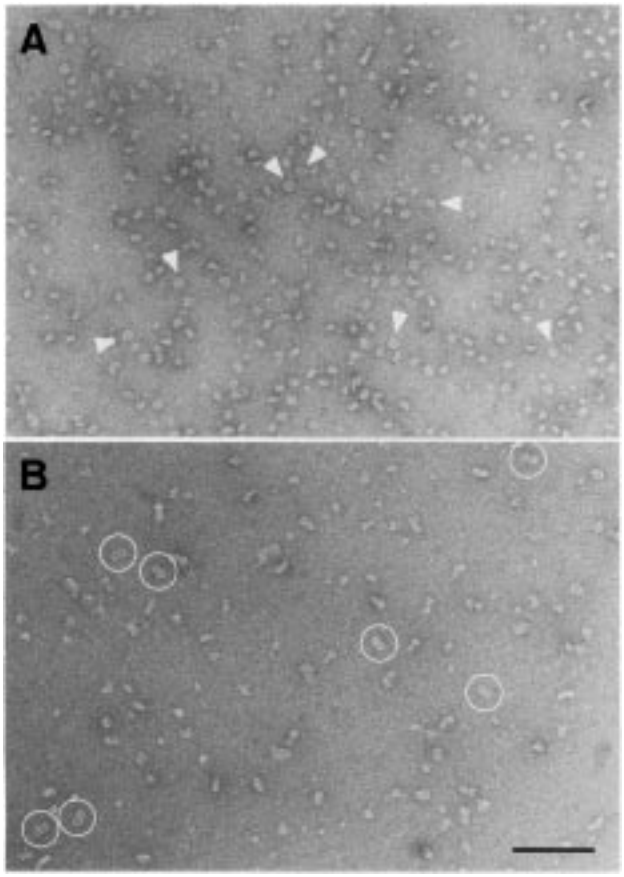

FIGURE 5: Electron micrographs of isolated $PMC3_{WT}$ (A) and $PMC4_{WT}$ (B). Isolated complexes were fixed with 10 mM glutaraldehyde, washed with 50 mM glygly, pH 7.8, to decrease the detergent and sucrose concentration, and stained with 2% uranyl acetate. Some presumed top views of monomeric RC−LH1 complexes are marked with arrowheads; some presumed top views of dimeric core complexes are encircled. Bar = 100 nm.

$PMC4_{WT}$ Can Be Converted into $PMC3_{WT}$. To confirm the proposed dimeric nature of $PMC4_{WT}$, we asked whether $PMC4_{WT}$ can be converted into $PMC3_{WT}$ by increasing amounts of detergent. The rationale of this experiment was that detergent molecules might destabilize hydrophobic interactions which are responsible for the formation of dimeric RC−LH1 complexes.

Isolated $PMC3_{WT}$ and $PMC4_{WT}$ were concentrated by ultrafiltration (see Materials and Methods) and loaded onto sucrose density gradients containing 0.2% sodium cholate and increasing concentrations of OG. As shown in Figure 6 (tubes 1 and 2), the sedimentation behavior of $PMC3_{WT}$ and $PMC4_{WT}$ is unchanged after concentration and recentrifugation over a sucrose gradient containing 0.6% OG. This result demonstrates that both complexes are stable enough to withstand ultrafiltration and a second round of rate zonal centrifugation. $PMC3_{WT}$ is stable even at 1.2% OG (Figure 6, tube 6), suggesting that $PMC3_{WT}$ corresponds to the classical RC−LH1 complex.

Interestingly, a stepwise increase of the OG concentration in the gradient (up to 1.2%) converts more and more $PMC4_{WT}$ into $PMC3_{WT}$ (Figure 6, tubes 3−5). Therefore, $PMC4_{WT}$ is indeed built of the same minimal units as

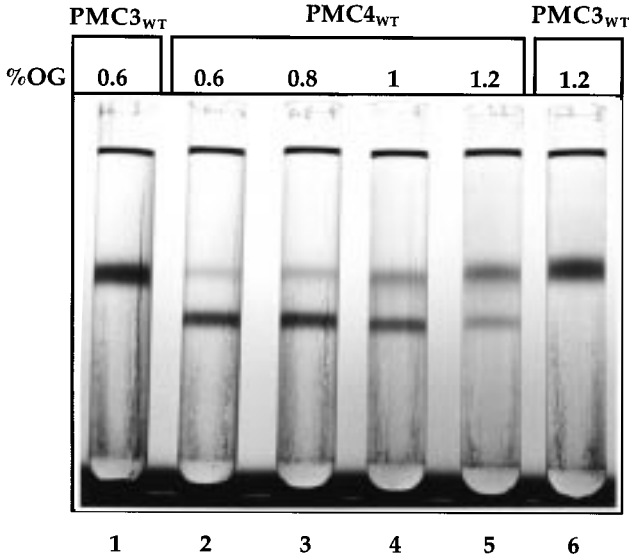

FIGURE 6: Sedimentation analysis of $PMC3_{WT}$ and $PMC4_{WT}$. The PMCs were isolated from photosynthetically grown ΔQ-X/g ($pRKXHis_6$) cells, concentrated by ultrafiltration (see Materials and Methods), and reloaded onto a 10−40% (w/w) sucrose gradient containing 0.2% sodium cholate and 0.6, 0.8, 1.0, or 1.2% OG.

$PMC3_{WT}$, strongly supporting the hypothesis that $PMC4_{WT}$ is an oligomeric form of $PMC3_{WT}$.

DISCUSSION

In this study, we have shown that both native ICM as well as isolated RC−LH1 complexes contain one PufX-His_6 molecule per RC. This stoichiometry is independent of the growth conditions, suggesting that it is tightly regulated. In addition, the stoichiometry is not influenced by the chromosomal vs plasmid-borne localization of the *puf* operon, thus excluding the possibility of polar effects influencing the number of PufX molecules per RC. The tightly fixed PufX/RC stoichiometry is consistent with the fact that *puf*X is transcribed as part of the same polycistronic mRNA as the RC genes *puf*L and *puf*M.

Following gentle solubilization of the ICM with a specific mixture of detergents (OG and sodium cholate), a characteristic pattern of carotenoid-containing membrane complexes was obtained. As described previously (*34*), the membrane complex with the lowest molecular weight (PMC1) consists mainly of LH2. In contrast, PMC2 is composed mainly of LH1, suggesting that this complex corresponds to mostly empty LH1 rings which have lost their RC core. Interestingly, however, both PMC1 and PMC2 preparations still contain traces of RC (see Table 2). The bchl/RC ratio of PMC2, for example, indicates the presence of 1 RC for every 5−6 LH1 rings (assuming 32 bchl molecules for each LH1 ring) (*4*). When the sucrose gradients shown in Figure 2 were harvested continuously and all fractions were analyzed by SDS−PAGE and silver staining, we found that RC traces comigrate with PMC1 and PMC2 on sucrose gradients (not shown). This result is consistent with a recent study in which 'free RC' was detected between 10% and 20% sucrose on solubilization and purification of photosynthetic membrane complexes (*21*).

In addition to the low levels of RC, $PMC2_{WT}$ is also partially associated with PufX. Interestingly, the PufX/RC stoichiometry was reproducibly found to be around 2, suggesting that the PufX-LH1 interaction is stronger than the RC binding to the LH1 ring. This interpretation is consistent with models suggesting that PufX is part of the LH1 ring (see below).

Under the specific detergent conditions used here, we have identified two membrane complexes ($PMC3_{WT}$ and $PMC4_{WT}$) which differ drastically in their sedimentation coefficients but have very similar subunit compositions. $PMC4_{WT}$ was only observed when the sucrose gradient contained 0.2% sodium cholate and OG concentrations below 1%. Therefore, very specific extraction conditions are required to allow isolation of this membrane complex. Interestingly, both $PMC3_{WT}$ and $PMC4_{WT}$ are composed of RC−LH1 cores, as judged by their absorption profiles, by their protein pattern in SDS gels, and by their stoichiometric bchl/RC and PufX/RC ratios. In addition, $PMC3_{WT}$ and $PMC4_{WT}$ display very similar levels of saturation in RC photobleaching experiments, suggesting that LH1 was still coupled to the RC in the isolated complexes (approximately 90% of RC photooxidation after the first of 10 actinic flashes; not shown). In fact, analogous measurements performed on RC deprived of LH1 resulted in a dramatically lower level of saturation (approximately 40% after the first flash vs 90% in RC−LH1 complexes; not shown).

The bchl/RC ratios in Table 2 are consistent with previously published values for the LH1/RC stoichiometry. Based on different techniques including electron microscopic analysis of 2D crystals, 16 α/β subunits of LH1 have been suggested to surround the RC in many purple bacteria (*3*, *11*). Although lower numbers have also been described, the model of a 16-meric LH1 ring is strengthened by the prediction that only the $\alpha_{16}\beta_{16}$ ring is large enough to accommodate a RC in its center (*4*). Furthermore, the diameter of the LH1 ring (11−12 nm) was found to be very similar in several species (*11*, *39*, *43*, *44*), suggesting that most LH1 antennae might be composed of 16 α/β subunits. This interpretation is supported by the bchl/RC ratio measured for $PMC3_{WT}$ (see Table 2). Taking into account the 4 bchl molecules of the RC itself, $PMC3_{WT}$ contains 16.4 ± 0.7 α/β subunits per RC, consistent with our conclusion that $PMC3_{WT}$ corresponds to a monomeric RC−LH1 complex. In contrast, the LH1/RC stoichiometry of $PMC3_{\Delta X}$ is increased to 17.8 ± 1.3 (see Table 2, again considering the bchl molecules in the RC). This is consistent with previous observations that deletion of *puf*X induces a small, but significant, increase in the LH1/RC stoichiometry (*16*, *18*−*20*, *45*). As suggested before, this increase is probably caused by the substitution of PufX by additional LH1 subunits (*19*, *20*, *45*).

Gel filtration experiments revealed that the two forms of the core complexes have significantly different molecular masses (PMC4/PMC3 = 1.59). The expected molecular mass of a RC−LH1 complex is 350 kDa, based on the masses of the RC (100 kDa), 1 PufX protein (10 kDa), and a ring composed of 16 $\alpha\beta$ heterodimers each containing 2 bchl and 2 carotenoids ($16 \times 15 = 240$ kDa). Using gel filtration, an apparent molecular mass of about 470 kDa was measured for $PMC3_{WT}$. The difference between the expected and the observed mass (120 kDa) is most likely due to detergent molecules interacting with outer hydrophobic surface of the RC−LH1 complex. For $PMC4_{WT}$, an apparent molecular mass of 750 kDa was determined by gel filtration. Although

gel filtration separates molecules not only due to their mass, but also due to their shape, this value is consistent with the interpretation of a dimeric core complex composed of 2 RCs (200 kDa), 2 PufX molecules (20 kDa), and approximately 27 LH1 subunits (derived from the bchl/RC stoichiometry in Table 2; $27 \times 15 = 405$ kDa). Interestingly, this number of LH1 subunits is significantly lower than double of that found for $PMC3_{WT}$. This result is consistent with the shape of $PMC4_{WT}$ observed by electron microscopy. Apparently, the LH1 antenna of the dimeric core complex is built of two tightly intertwined LH1 rings, thus forming an "eight-like" structure with a reduced number of LH1 subunits at the contact site. Similarly, the remaining mass of $PMC4_{WT}$ (about 125 kDa, attributed to detergent) is significantly lower than that for two $PMC3_{WT}$ complexes, indicating that the monomer−monomer interaction significantly reduced the hydrophobic surface available to detergent molecules. However, it has to be kept in mind that these numbers are only rough estimates of the PMCs composition, due to the different shapes of the monomeric and dimeric core complexes.

The question arises as to whether the RC−LH1 complex exists as a dimer in vivo. Several independent lines of evidence indicate that dimeric RC−LH1 complexes are present in native membranes, and not the consequence of dimerization of the His_6-tag or detergent-induced aggregation in vitro: (1) The possibility of a His_6-tag-induced dimerization is clearly excluded by the fact that dimeric core complexes were also isolated from strains carrying an untagged *puf*X gene (Barz and Francia, unpublished results). (2) Following solubilization of the ICM, the spectroscopic properties of the LH1 antennae in the detergent extracts are very similar to those in the native membranes (Figure 3B), indicating that the aggregation state of LH1 was not radically altered during the solubilization procedure. (3) Addition of a molecular excess of purified PufX-His_6 to preparations of $PMC3_{\Delta X}$ did not allow reconstitution of a dimeric core complex (gradient not shown), indicating that these dimers cannot be formed spontaneously under these in vitro conditions, but only under more physiological conditions. (4) Interestingly and most convincingly, a dimeric core complex has recently been observed in native membranes of a *Rb. sphaeroides* strain lacking LH2 antennae (*15*). In that study, the structure of the photosynthetic unit was determined at 20 Å resolution using electron microscopy of two-dimensional crystals in their native membrane. The projection map revealed a "S-shaped" structure composed of two incomplete antenna rings, each having a diameter of about 120 Å and containing an electron-dense nucleus attributed to the RC. Interestingly, the openings in the LH1 rings surrounding the RCs directly confirm previous suggestions that the native LH1 structure must contain opening(s) to allow a fast lateral ubiquinone/ubiquinol exchange between the RC and the cyt bc_1 complex (*19*, *25*).

In contrast to the detergent-solubilized RC−LH1 dimers found in this study, the native photosynthetic unit contains stoichiometric amounts of the cyt bc_1 complex (*15*). This difference can be explained by the well-established extraction of the cyt bc_1 complex in the first solubilization step (*34*). The absence of the cyt bc_1 complex from the PMCs was clearly confirmed by the protein pattern in SDS gels (Figure 4). Therefore, it is conceivable that photosynthetic core complexes are in close contact with cyt bc_1 complexes in native membranes, possibly even in the presence of LH2 antennae (*46*), but that this interaction is too weak to withstand the detergent extraction used in this study.

The fact that both monomeric and dimeric core complexes were isolated from ΔQ-X/g (pRKXHis_6) and ΔQ-X/g (pRKX) membranes raises the question whether both of these forms exist in native membranes. Alternatively, the RC−LH1 dimer could be the only physiological form in vivo and the monomer could be the product of detergent-induced dimer dissociation. Since monomerization of the dimeric core was observed at increasing detergent concentration (Figure 6), we favor the idea that the dimeric core is the preferred arrangement in vivo. During membrane solubilization of the PMCs, the detergent molecules compete with LH1 molecules for the hydrophobic membrane sites of the monomer, thus explaining the co-isolation of monomeric $PMC3_{WT}$ and dimeric $PMC4_{WT}$. This interpretation is supported by the observation that an increased OG concentration prevents the isolation of $PMC4_{WT}$ (Barz and Francia, unpublished results), consistent with the fact that dimeric core complexes have not been described in previous solubilization studies. Although these results are consistent with a predominantly dimeric nature of core complexes in vivo, a simultaneous occurrence of both RC−LH1 forms in native membranes cannot be excluded from the present data.

The dimeric nature of $PMC4_{WT}$ is consistent with the proposal that the elements of the photosynthetic apparatus may be organized in supercomplexes, each containing two RCs, one cyt c_2 and one cyt bc_1 complex (*46*). This suggestion originated from spectroscopic studies on intact *Rb. sphaeroides* cells, showing that the apparent equilibrium constant between the different reactants, measured during photooxidation of the donor chain under continuous illumination, was much lower than that deduced from their midpoint potentials measured at equilibrium (*46*).

Most excitingly, the isolation of the dimeric core complex is strictly dependent on the presence of PufX (Figure 2). Under all conditions tested, such a high molecular weight complex was not observed in more than 10 sucrose density gradients that were performed with detergent extracts of the *puf*X-deleted strain. Therefore, PufX seems to be a key factor in the formation of the dimeric RC−LH1 complex. Since the presence of PufX is also essential for efficient ubiquinone/ubiquinol exchange (*25*), we propose that dimer formation is important for photosynthetic competence. This functional requirement for dimerization could be explained by two alternative molecular models: first, dimer formation could be essential to form specific openings in the LH1 ring structure, thus allowing an efficient lateral ubiquinone/ubiquinol transfer through the antenna ring. This model is consistent with previous studies suggesting that PufX limits the aggregation state of LH1 antennae (*18*) and that PufX is required to prevent the physical blockage of the RC Q_B site by LH1 unless the stoichiometric LH1/RC ratio is significantly reduced by LH1 mutations (*23*, *45*). Alternatively, PufX could simply act as a "symmetry breaker" to prevent the clustering of RC−LH1 complexes into large aggregates. Such a clustering of monomeric core complexes into a hexagonal arrangement has been observed for several species of purple bacteria lacking PufX (*43*, *44*). Due to this second model, PufX-induced core dimerization would indirectly facilitate the functional interplay of RC−LH1 cores with

other components of the photosynthetic unit (like LH2 antenna and cyt bc_1 complexes).

Since these models are not mutually exclusive, PufX might facilitate light-induced cyclic electron transfer by both forming a hole in the LH1 ring and preventing symmetrical RC−LH1 aggregates. In any case, PufX seems to play a structural role in forming an asymmetrical arrangement of LH1 around the RC. Therefore, the RC−LH1 core of *Rb. sphaeroides* may be an exception of the circular symmetry which is usually a prominent feature of antenna complexes. Interestingly, another example for a noncircular antenna structure was recently observed in *Rs. rubrum*, where image analysis of 2D crystals of RC−LH1 complexes has revealed an almost square LH1 structure (*47*). Furthermore, this unusual antenna structure was found to contain a small protein called W. Although the primary structure of W does not resemble that of PufX, this results supports our suggestion that a small transmembrane protein can alter the structure of the antenna surrounding the RC.

An asymmetric LH1 organization in *Rb. sphaeroides* could possibly explain the nature of 'B896', a rare antenna pigment absorbing at 896 nm (*48*). Since the presence of B896 is an inherent property of the LH1 complex, it is believed to be a subspecies of LH1 (48). Interestingly, deletion of PufX was found to change the oligomerization state of the LH1 ring as well as a spectral red shift of the fluorescence polarization of B896, suggesting that the presence of B896 requires a limited aggregation state of the LH1 antennae (*18*). Since some LH1 subunits in the dimeric RC−LH1 complex (i.e., those next to an opening in the LH1 ring) are likely to have different absorption characteristics than others, we propose that this break in the LH1 symmetry could be the structural basis for the B896 subspecies of LH1.

ACKNOWLEDGMENT

We are grateful to Boris Bieger for help with gel filtration experiments and to Rita Wiemeyer for perfect technical assistance. We also thank Ute Santarius for taking the electron micrographs, Matteo Conti, Miro Venturi, and Luca Lambertini for their help during the establishment of the PMC isolation procedure, and André Verméglio for communicating related results prior to publications.

REFERENCES

1. Kiley, P. J., and Kaplan, S. (1988) *Microbiol. Rev. 52*, 50−69.
2. Cohen-Bazire, G., Sistrom, W. R., and Stanier, R. Y. (1957) *J. Cell. Comput. Physiol. 49*, 25−68.
3. Gall, A. (1995) Ph.D. Thesis, University of Glasgow, Glasgow, U.K.
4. Cogdell, R. J., Fyfe, P. K., Barrett, S. J., Prince, S. M., Freer, A. A., Isaacs, N. W., McGlynn, P., and Hunter, C. N. (1996) *Photosynth. Res. 48*, 55−63.
5. Aagaard, J., and Sistrom, W. R. (1972) *Photochem. Photobiol. 15*, 299−225.
6. Hawthornthwaite, A. M., and Cogdell, R. J. (1991) in *The Chlorophylls* (Scheer, H., Ed.) pp 493−528, CRC Press Inc., Boca Raton, FL.
7. Deisenhofer, J., and Michel, H. (1989) *EMBO J. 8*, 2149−2170.
8. Rees, D. C., Komiya, H., Yeates, T. O., Allen, J. P., and Feher, G. (1989) *Annu. Rev. Biochem. 58*, 607−633.
9. McDermott, G., Prince, S. M., Freer, A. A., Hawthornthwaite-Lawles, A. M., Papiz, M. Z., Cogdell, R. J., and Isaacs, N. W. (1995) *Nature 374*, 517−521.
10. Koepke, J., Hu, X., Muenke, C., Schulten, K., and Michel, H. (1996) *Structure 4*, 581−597.
11. Karrasch, S., Bullough, P., and Ghosh, R. (1995) *EMBO J. 14*, 631−638.
12. Papiz, M. Z., Prince, M. S., Hawthornthwaite-Lawless, A. M., McDermott, G., Freer, A. A., Isaacs, N. W., and Cogdell, R. J. (1996) *Trends Plant Sci. 1*, 198−206.
13. Hu, X., and Schulten, K. (1997) *Physics Today 50*, 28−34.
14. Hu, X., Ritz, T., Damjanovic, A., and Schulten, K. (1997) *J. Phys. Chem. B 101*, 3854−3871.
15. Jungas, C., Ranck, J.-L., Rigaud, J.-L., Joliot, P., and Verméglio, A. (1999) *EMBO J.* (in press).
16. Farchaus, J. W., Barz, W. P., Grünberg, H., and Oesterhelt, D. (1992) *EMBO J. 11*, 2779−2788.
17. Lilburn, T. G., Haith, C. E., Prince, R. C., and Beatty, J. T. (1992) *Biochim. Biophys. Acta 1100*, 160−170.
18. Westerhuis, W. H. J., Farchaus, J. W., and Niederman, R. A. (1993) *Photochem. Photobiol. 58*, 460−463.
19. McGlynn, P., Hunter, C. N., and Jones, M. R. (1994) *FEBS Lett. 349*, 349−353.
20. Barz, W. P., Francia, F., Venturoli, G., Melandri, B. A., Verméglio, A., and Oesterhelt, D. (1995) *Biochemistry 34*, 15235−15247.
21. Pugh, R. J., McGlynn, P., Jones, M. R., and Hunter, C. N. (1998) *Biochim. Biophys. Acta 1366*, 301−316.
22. Recchia, P. A., Davis, C. M., Lilburn, T. G., Beatty, J. T., Parkes-Loach, P. S., Hunter, C. N., and Loach, P. A. (1998) *Biochemistry 37*, 11055−11063.
23. Barz, W. P., and Oesterhelt, D. (1994) *Biochemistry 33*, 9741−9752.
24. Lilburn, T. G., Prince, R. C., and Beatty, J. T. (1995) *J. Bacteriol. 177*, 4593−4600.
25. Barz, W. P., Verméglio, A., Francia, F., Venturoli, G., Melandri, B. A., and Oesterhelt, D. (1995) *Biochemistry 34*, 15248−15258.
26. Sistrom, W. R. (1960) *J. Gen. Microbiol. 22*, 778−785.
27. Martin, J. P. Jr., Colina, K., and Logsdon, N. (1987) *J. Bacteriol. 169*, 2516−2522.
28. Sambrook, J., Fritsch, E. F., and Maniatis, T. (1989) *Molecular cloning: A laboratory manual*, Cold Spring Harbor Laboratory Press, Cold Spring Harbor, NY.
29. Simon, R., Priefer, U., and Pühler, A. (1983) *Bio/Technology 1*, 784−791.
30. Davis, J., Donohue, T. J., and Kaplan, S. (1988) *J. Bacteriol. 170*, 320−329.
31. Ditta, G., Schmidhauser, T., Yakobson, E., Lu, P., Liang, X. W., Finlay, D. R., Guiney, D., and Helinski, D. R. (1985) *Plasmid 13*, 149−153.
32. Bowyer, J. R., Tierney, G. V., and Crofts, A. R. (1979) *FEBS Lett. 101*, 201−206.
33. Schägger, H., and von Jagow, G. (1987) *Anal. Biochem. 166*, 368−379.
34. Gabellini, N., Gao, Z., Oesterhelt, D., Venturoli, G., and Melandri, B. A. (1989) *Biochim. Biophys. Acta 974*, 202−210.
35. Clayton, R. K. (1966) *Photochem. Photobiol. 5*, 669−677.
36. Venturoli, G., Fernández-Velasco, J. G., Crofts, A. R., and Melandri, B. A. (1986) *Biochim. Biophys. Acta 851*, 340−352.
37. Dutton, P. L., Petty, K. M., Bonner, H. S., and Morse, S. D. (1975) *Biochim. Biophys. Acta 387*, 536−556.
38. Bowyer, J. R., Meinhardt, S. W., Tierney, G. V., and Crofts, A. R. (1981) *Biochim. Biophys. Acta 635*, 167−186.
39. Boonstra, A. F., Germeroth, L., and Boekema, E. J. (1994) *Biochim. Biophys. Acta 1184*, 227−234.
40. Bevington, P. R. (1969) *Data Reduction and Error Analysis for the Physical Science*, McGraw-Hill, New York.
41. Farchaus, J. W., Grünberg, H., and Oesterhelt, D. (1990) *J. Bacteriol. 172*, 977−985.
42. Loach, P. A., and Parkes-Loach, P. S. (1995) in *Anoxygenic Photosynthetic Bacteria* (Blankenship, R. E., Madigan, M. T.,

and Bauer, C. E., Eds.) pp 437−471, Kluwer Academic Publishers, Dordrecht, The Netherlands.
43. Stark, W., Kühlbrandt, W., Wildhaber, I., Wehrli, E., and Mühlethaler, K. (1984) *EMBO J. 3*, 777−783.
44. Meckenstock, R. U., Krusche, K., Staehelin, L. A., Cyrklaff, M., and Zuber, H. (1994) *Biol. Chem. Hoppe-Seyler 375*, 429−438.
45. McGlynn, P., Westerhuis, W. H. J., Jones, M. R., and Hunter, C. N. (1996) *J. Biol. Chem. 271*, 3285−3292.
46. Joliot, P., Verméglio, A., and Joliot, A. (1989) *Biochim. Biophys. Acta 975*, 336−345.
47. Stahlberg, H., Dubochet, J., Vogel, H., and Ghosh, R. (1998) *Photosynth. Res. 55*, 363−368.
48. Kramer, H. J. M., Pennoyer, J. D., van Grondelle, R., Westerhuis, W. H. J., Niederman, R. A., and Amesz, J. (1984) *Biochim. Biophys. Acta 767*, 335−344.

BI982891H